Carbazole Based Anionic MOF for Proton Conductivity①

GUO Shan-Shan[a] HUANG Lv-Lan[a] YE Ying-Xiang[a]
LIU Li-Zhen[a] YAO Zi-Zhu[a] XIANG Sheng-Chang[a, b]
ZHANG Jin-Dan[a] ZHANG Zhang-Jing[a, b②]

[a] (*College of Chemistry and Materials Science, Fujian Provincial Key Laboratory of Polymer Materials, Fujian Normal University, Fuzhou* 350007, *China*)

[b] (*State Key Laboratory of Structural Chemistry, Fujian Institute of Research on the Structure of Matter, Chinese Academy of Sciences, Fuzhou* 350002, *China*)

ABSTRACT A non-interpenetrated anionic In-MOF (**FJU-302**) based on a linear H_2bpdc and an angled H_2cdc as dual-ligands was characterized by FT-IR, TGA and X-ray single-crystal/powder diffraction. **FJU-302** crystallizes in the monoclinic system and $I4_1/amd$ space group with a = 27.1274(8), b = 27.1274(8), c = 29.788(3) Å, V = 21921(2) Å^3, Z = 16, M_r = 608.32, D_c = 0.737 g/cm^3, $F(000)$ = 4848, μ(Cu$K\alpha$) = 3.659 mm^{-1}, R = 0.0800 and wR = 0.1911 for 5703 observed reflections ($I > 2\sigma(I)$), and R = 0.1470 and wR = 0.2342 for all data. In this work, a carbazole based anionic In-MOF (**FJU-302**) was designed and synthesized, and the proton conductivity from subzero temperature (–30 °C) to 70 °C was measured without additional humidity. **FJU-302** presents a max proton conductivity of 6.47 × 10^{-4} S·cm^{-1} at 70 °C, and it can maintain 5.88 × 10^{-7} S·cm^{-1} at –30 °C. This work reports a first carbazole based MOF for proton conductivity at subzero temperature conditions.

Keywords: **metal-organic frameworks, carbazole, proton conductivity;**
DOI: 10.14102/j.cnki.0254-5861.2011-2761

1 INTRODUCTION

Carbazole based carboxylic acid has been used as bridge ligands to construct a variety of metal-organic frameworks (MOFs) due to the coplane structure leading to excellent conjugacy and rigidity and the surplus N site[1, 2]. Among them, 9H-carbazole-3,6-dicarboxylate (H_2cdc) attracts attention for the unique angle of 90° between the planes of carboxylic groups[1]. In previous work, the H_2cdc based MOFs have been synthesized for the application in gas capture[1]~[7]. However, the work on the proton conductivity of this type of MOFs is barely reported. Generally, proton conductivity of MOFs arises from the incorporating functional groups (such as carboxylic, sulfonic, phosphonic, or hydroxyl groups) and guest proton carrier species (e.g. water, acid, imidazole, H_3O^+, NH_4^+, Emim$^+$, etc.) in the pores of MOFs[8]~[11]. To further improve the proton conductivity of MOFs, constructing large void space in MOFs containing more guest proton carriers is a feasible strategy[12]. Therefore, considering the obtained high porosity of H_2cdc based MOFs in previous work, such as DUT-49 (porosity of 84.7% by PLATON, the same below)[13], DUT-76 (86.0%)[14], $[Cu_2(cdc)_2(DMA)(EtOH)]_6{\cdot}x$S (76%)[15] and $[(Cu_2)_9$(9H-3,6-cdc$)_6$(pddb$)_{12}$(DMA$)_6$($H_2O)_{12}]{\cdot}x$S (75%)[16], carbazole based MOFs have potential to be applied as solid state proton conductors, which lie at the foundation of many energy-related applications like batteries and fuel cells[17~19].

Herein, a dual-ligand indium(III)-based MOF ($[(CH_3)_2NH_2][In(cdc)(bpdc)]\cdot 4DMF\cdot 2H_2O$ (**FJU-302**)) with cdc ligand was synthesized for proton conductivity. The indium metal was chosen for their well-known tendency to form a charged secondary building unit (SBU), and the anionic MOFs with charging-balancing cations outside the framework are the best choice for proton conductivity in MOF family[20]~[21]. In this condition, a second ligand 4,4′-biphenyldicarboxylic acid (H_2bpdc) is used, for its long

Received 10 February 2020; accepted 29 February 2020 (**CCDC 1976903**)

① This work was supported by the National Natural Science Foundation of China (21673039, 21573042, 21805039, 21975044 and 21971038), the Fujian Provincial Department of Science and Technology (2018J07001 and 2019H6012), and Education Department of Fujian province (JT180090)

② Corresponding author. E-mails: scxiang@fjnu.edu.cn, zhangjindan@fjnu.edu.cn and zzhang@fjnu.edu.cn

and slim structure would help build more large void space[1]. The synthesized MOF has a layer structure with a negative charged $[In(cdc)(bpdc)]^-$ layer with a porosity of 65.3%. To avoid the effects of water on the proton conductivity at subzero temperature, the impedance measurement of **FJU-302** was measured over a wide temperature range from subzero (–30 °C) to moderate temperature (70 °C) without additional humidity. Results show that **FJU-302** presents an proton conductivity of 5.88×10^{-7} at –30 °C, and the value increases to 6.47×10^{-4} S·cm^{-1} at 70 °C. The derived activation energy (E_a) from impedance measurement is 0.568 eV, demonstrating vehicular mechanism of proton transportation in **FJU-302**.

2 EXPERIMENTAL

2. 1 Syntheses of 9H-carbazole-3,6-dicarboxylic acid (H_2cdc)

All reagents and solvents were commercially available and used as supplied without further purification. H_2cdc was synthesized by a modified literature method[22]: a mixture of carbazole (5.2 g, 30 mmol), chlorobenzene (100 mL), trichloroacetonitrile (7.5 mL, 75 mmol), and anhydrous aluminum chloride (10.6 g, 80 mmol) was treated with dry hydrogen chloride for 5 h. Throughout this, the mixture was stirred violently at 0 °C to give black mobile suspension. After that, the system was heated and stirred at 60 °C for 30 min, then 100 °C for 2 h and lastly boiled for 2 h to give a black solid. After cooling to room temperature, the reaction mixture was treated with 25 mL concentrated hydrochloric acid. After the vigorous reaction subsided, the mixture was boiled again with stirring for 5 h. The mixture was concentrated under reduced pressure to remove chloro-benzene and most of HCl to give a black solid. This solid was refluxed in 150 mL of 2.5 M aqueous KOH for 2 h and treated with active carbon for an additional 2 h. After cooling to room temperature, the mixture was treated with 50 mL 5 M aqueous HCl, and the yellow precipitate was filtered. The precipitate was collected, washed with water for several times until pH = 7, and then dried at 80 °C to give the title compound as light-yellow powder (45% yield). 1H-NMR (DMSO-d6): δ = 12.07 (s, 1 H), 8.8 (s, 2 H), 8.06(d, 2 H), 7.6 (d, 2 H).

2. 2 Syntheses of $[(CH_3)_2NH_2][In(cdc)(bpdc)]\cdot 4DMF\cdot 2H_2O$ (FJU-302)

A mixture of $In(NO_3)_3\cdot xH_2O$ (18.5 mg), 4,4′-biphenyldicarboxylic acid (24.00 mg), H_2cdc (25.5 mg), N,N-dimethylformamide (DMF, 4 mL) and H_2O (1 mL) in a Teflon-lined autoclave was sealed and heated at 120 °C for 120 h. The light yellow block-shaped crystal was obtained after filtration and dry. Elemental analysis: C, 50.67; H, 4.66; N, 8.82%. Calculated results: C, 51.37; H, 5.50; N, 8.56%.

2. 3 Characterization

Powder X-ray diffraction (PXRD) was carried out with a PANalytical X'Pert3 powder diffractometer equipped with a Cu sealed tube (λ = 1.541874 Å) at 40 kV and 40 mA over the 2θ range of 5～30°. Thermal analysis was carried out on a METTLER TGA/SDTA 851 thermal analyzer from 30 to 600 ℃ at a heating rate of 10 °C·min^{-1} under nitrogen atmosphere. The Fourier transform infrared (KBr pellets) spectra were recorded in the range of 400～4000 cm^{-1} on a Thermo Nicolet 5700 FT-IR instrument.

2. 4 AC Impedance

The alternating current (AC) impedance test from –30 to 70 °C was recorded with a 1296 Dielectric Interface Impedance Analyzer over the frequency range of 100 Hz to 1 MHz. The measurement procedure was similar to our pervious report[18, 19, 22]. The as-synthesized sample was finely ground and compressed into a circular cylinder. Proton conductivity (σ) was calculated by using σ = l/SR, where l and S are the length (cm) and cross-sectional area (cm^2) of the compressed samples, and R is the bulk resistance. Activation energy (E_a) was estimated from the following equation:

$$\sigma T = \sigma_0 exp(-\frac{E_a}{k_B T})$$

where σ is the proton conductivity, σ_0 the pre-exponential factor, k_B the Boltzmann constant, and T the temperature (K). The Impedance data were analyzed by using ZView software.

2. 5 Single-crystal X-ray structural analysis

Data collection and structural analysis of crystal **FJU-302** were performed on an Agilent Technologies SuperNova single crystal diffractometer equipped with graphite-monochromatic Cu$K\alpha$ radiation (λ = 1.5406 Å). The crystal was kept at 293 and 100 K during data collection. Using Olex2[23], the structure was solved with the Superflip[24] structure solution program using charge flipping and refined with the ShelXL[25] refinement package with the least-squares minimization. All non-hydrogen atoms were refined with anisotropic displacement parameters. The hydrogen atoms on the ligands were placed at idealized positions and refined using a riding model. PLATON[26] and SQUEEZE[27] were

employed to calculate the diffraction contribution of the solvent molecules and thereby produce a set of solvent-free diffraction intensities. The relevant crystal data and structural refinement parameters are listed in Tables S1. Selected bond and angle parameters are listed in Table 1.

Table 1. Selected Bond Lengths (Å) and Bond Angles (°) for FJU-302

Bond	Dist.	Bond	Dist.	Bone	Dist.
O(2)–In(1)	2.260(5)	O(7)–In(1)	2.231(5)	In(1)–O(2)^1	2.260(6)
O(4)–In(1)	2.314(6)	O(8)–In(1)	2.286(6)	In(1)–O(4)^1	2.314(6)
In(1)–O(7)^1	2.231(5)	In(1)–O(8)^1	2.286(6)		
Angle	(°)	Angle	(°)	Angle	(°)
O(4)^1–In(1)–O(4)	89.4(3)	O(7)^1–In(1)–O(2)	85.9(2)	O(7)^1–In(1)–O(2)^1	136.0(3)
O(7)–In(1)–O(2)^1	85.9(2)	O(7)–In(1)–O(2)	136.0(3)	O(7)–In(1)–O(4)^1	167.8(2)
O(7)–In(1)–O(4)	92.1(2)	O(7)–In(1)–O(4^1)	92.1(2)	O(7)^1–In(1)–O(4)	167.8(2)
O(7)–In(1)–O(8)	57.9(2)	O(7)^1–In(1)–O(8)	91.5(2)	O(7)^1–In(1)–O(8)^1	57.9(2)
O(7)–In(1)–O(8)^1	91.5(2)	O(2)–In(1)–O(2)^1	125.8(4)	O(2)–In(1)–O(4)^1	56.1(2)
O(2)^1–In(1)–O(4)	56.1(2)	O(2)^1–In(1)–O(4)^1	84.8(2)	O(2)–In(1)–O(4)	84.8(2)
O(2)^1–In(1)–O(8)	121.4(2)	O(2)–In(1)–O(8)	78.6(2)	O(2)^1–In(1)–O(8)^1	78.6(2)
O(2)–In(1)–O(8)^1	121.4(2)	O(8)–In(1)–O(4)	78.9(2)	O(8)^1–In(1)–O(4)	134.2(2)
O(8)^1–In(1)–O(4)^1	78.9(2)	O(8)–In(1)–O(4)^1	134.2(2)	O(8)^1–In(1)–O(8)	138.4(3)

Symmetry code: ^{1} 3/4–*y*, 3/4–*x*, 5/4–*z*

Table 2. Correlation Index of π-π Interactions[a]

	Centroid distance (Å)	Perpendicular distance (Å)	Dihedral angle
a axis	4.131(12)	3.504(17)	0
b axis	4.131(12)	3.504(17)	0

[a] It has the same π-π interactions along axes *a* and *b* because **FJU-302** crystallizes in the tetragonal system.

3 RESULTS AND DISCUSSION

3. 1 Structure description

FJU-302 was synthesized with $In(NO_3)_3 \cdot xH_2O$, H_2cdc and 4,4′-biphenyldicarboxylic acid (H_2bpdc) as the first and second ligands. SCXRD reveals that **FJU-302** crystallizes in the tetragonal system and $I4_1/amd$ space group. The crystal structure of **FJU-302** can be understood as negative charged $[In(cdc)(bpdc)]^-$ layers with charge balancing cation $[(CH_3)_2NH_2]^+$ and neutral DMF, and H_2O guests locate at the interlayer space. The asymmetric unit of **FJU-302** consists of an In(III) ion, a bpdc and a cdc ligands. Each In(III) is octa-coordinated by eight oxygen atoms from four carboxylic acid groups of two bpdc ligands and two cdc ligands, forming a 4-chelated $[In(CO_2)_4]^-$ subunit (Fig. 1a). Four adjacent cdc ligands connect four $[In(CO_2)_4]^-$ subunits, giving rise to a 4-membered ring (ring type I in Fig. 1b). And a negative charged $[In(cdc)(bpdc)^-$ layer is formed by connecting four types of I rings by the second ligand bpdc, and thus three types of 4-membered rings (type I, II, III) are found in each layer due to the coexistence of two kinds of ligands (Fig. 1b). The layers stack along the *b* axis, forming a linear tunnel along the *c* axis with π-π interactions. The distance of each layer is 7.477 Å (Fig. 1c, d). The pore volume of **FJU-302** calculated by PLATON is 65.3%.

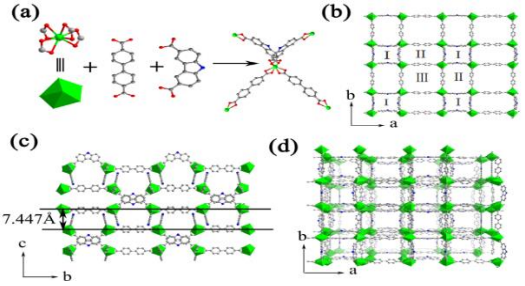

Fig. 1. Crystal structure of FJU-302. (a) Coordination environment of In atoms; (b) Negatively charged $[In(cdc)(bpdc]^-$ layers from *c* direction; (c) Layers stacked along the *b* axis; (d) Linear tunnel along the *c* axis

3. 2 Powder X-ray diffraction and thermogravimetric analysis

Power X-ray diffraction (PXRD) pattern of **FJU-302** is shown in Fig. S1a. The PXRD pattern of synthesized samples matches the simulated curves well, implying its complete structure and high purity. Thermogravimetric analysis (TGA) curves are presented in Fig. S1b. The result shows that the samples can keep their framework until 360 ℃ and the 40% weight loss before 295 ℃ can be ascribed to the loss of guest molecules at the interlayer space. Combined with SCXRD, elemental analysis (experimental part in supporting information) and TGA results, the molecular formula of **FJU-302** is determined as $[(CH_3)_2NH_2][In(cdc)(bpdc)]\cdot 4DMF\cdot 2H_2O$.

3. 3 Proton conductivity

To determine the proton conductivity of **FJU-302**, the alternating current (AC) impedance spectroscopy was performed on a compressed pellet of the crystalline powder sample coated with Ag electrodes without additional humidity at –30～70 ℃. The obtained Nyquist plot and proton conductivity are shown in Fig. 2 and Table S2.

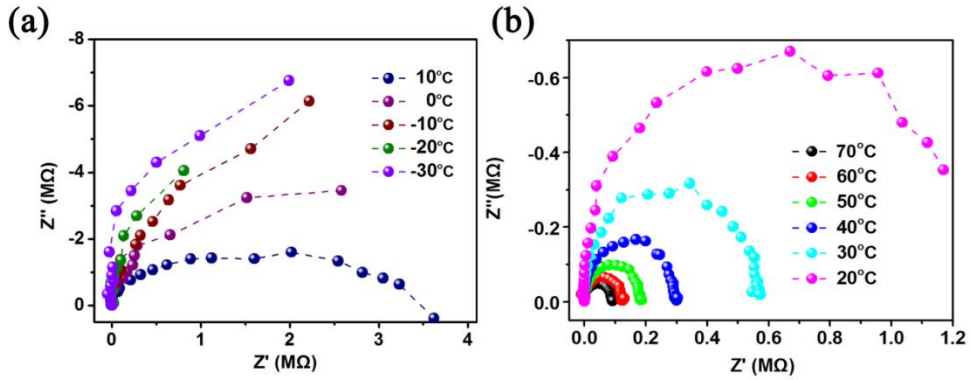

Fig. 2. Nyquist plots of FJU-302 at –30～70 ℃ without additional humidity

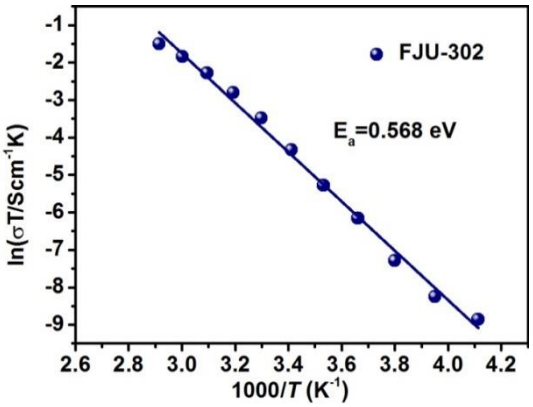

Fig. 3. Arrhenius plots of FJU-302 at –30～70 ℃ without additional humidity

The proton conductivity for **FJU-302** was found to be 5.88×10^{-7} and 1.01×10^{-4} $S\cdot cm^{-1}$ at –30 ℃ and 30 ℃, respectively. The conductivity increases with increasing temperature and reaches a maximum of 6.47×10^{-4} $S\cdot cm^{-1}$ at 70 °C. To explore the proton-conductivity mechanism, activation energy (E_a) is estimated from $\ln(\sigma T)$–1000 T^{-1} curve (Fig. 3). The least-squares fit of the Arrhenius plots yielded the activation energy value (E_a) of 0.568 > 0.4 eV, demonstrating a vehicular mechanism[18], namely, the proton carrier transports along the pores in framework even without any additional humidity, which supports the proton conductivity under freezing temperature[19].

4 CONCLUSION

In summary, a non-interpenetrated anionic In-MOF (**FJU-302**) was designed and synthesized with a linear H_2bpdc and an angled H_2cdc as dual-ligands. The synthesized **FJU-302** presents a stable layer structure with a negative charged $[In(cdc)(bpdc)]^-$ layer. The proton conductivity over a wide temperature range, especially at subzero temperature, was measured without additional humidity. Results show that **FJU-302** presents a max proton conductivity of 6.47×10^{-4} $S\cdot cm^{-1}$ at 70 ℃. And at –30 ℃, **FJU-302** can maintain a proton conductivity of 5.88×10^{-7} $S\cdot cm^{-1}$. The derived

activation energy (E_a = 0.568 eV) demonstrates a vehicular mechanism of proton carrier transportation in **FJU-302**.

REFERENCES

(1) Qin, Y.; Xue, M. H.; Dou, B.; Sun, Z.; Li, G. High protonic conduction in two metal-organic frameworks contained high-density carboxylic groups. *New J. Chem.* **2020**, 44, 2741–2748.

(2) Liu, R. L.; Shi, Z. Q.; Wang, X. Y.; Li, Z. F.; Li, G. Two highly stable proton conductive cobalt(II)-organic frameworks as impedancesensors for formic acid. *Chem. Eur. J.* **2019**, 25, 14108–14116.

(3) Lu, W. G.; Yuan, D. Q.; Makal, T. A.; Li, J. R.; Zhou, H. C. A highly porous and robust (3,3,4)-connected metal-organic framework assembled with a 90° bridging-angle embedded octacarboxylate ligand. *Angew. Chem. Int. Ed.* **2012**, 51, 1580–1584.

(4) Thomas, K. M. Adsorption and desorption of hydrogen on metal-organic framework materials for storage applications: comparison with other nanoporous materials. *Dalton Trans*. **2009**, 9, 1487–1505.

(5) Li, J. R.; Timmons, D. J.; Zhou, H. C. Interconversion between molecular polyhedra and metal-organic frameworks. *J. Am. Chem. Soc.* **2009**, 131, 6368–6369.

(6) Krause, S.; Bon, V.; Stoeck, U.; Senkovska, I.; Tçbbens, D. M.; Wallacher, D.; Kaskel, S. A stimuli-responsive zirconium metal-organic framework based on supermolecular design. *Angew. Chem. Int. Ed*. **2017**, 56, 10676–10680.

(7) Li, J. R.; Zhou, H. C. Bridging-ligand-substitution strategy for the preparation of metal-organic polyhedral. *Nat. Chem*. **2010**, 2, 893–898.

(8) Taylor, J. M.; Dekura, S.; Ikeda, R.; Kitagawa, H. Defect control to enhance proton conductivity in a metal-organic framework. *Chem. Mater*. **2015**, 27, 2286−2289.

(9) Umeyama, D.; Horike, S.; Inukai, M.; Kitagawa, S. Integration of intrinsic proton conduction and guest-accessible nanospace into a coordination polymer. *J. Am. Chem. Soc*. **2013**, 135, 11345−11350.

(10) Lai, X. Y.; Liu, Y. W.; Yang, G. C.; Liu, S. M.; Shi, Z.; Lu, Y.; Luo, F.; Liu, S. X. Controllable proton-conducting pathways *via* situating polyoxometalates in targeting pores of a metal-organic framework. *J. Mater. Chem. A* **2017**, 5, 9611−9617.

(11) Li, J. R.; Timmons, D. J.; Zhou, H. C. Interconversion between molecular polyhedra and metal-organic frameworks. *J. Am. Chem. Soc*. **2009**, 131, 18, 6368−6369.

(12) Liu, L. Z.; Yao, Z. Z.; Ye, Y. X.; Lin, Q. J.; Chen, S. M.; Zhang, Z. J.; Xiang, S. C. Enhanced intrinsic proton conductivity of metal-organic frameworks by tuning the degree of interpenetration. *Cryst. Growth Des*. **2018**, 18, 3724−3728.

(13) Stoeck, U.; Krause, S.; Bon, V.; Senkovska, I.; Kaskel, S. A highly porous metal-organic framework, fonstructed from a cuboctahedral super-molecular building block, with exceptionally high methane uptake. *Chem. Commun*. **2012**, 48, 10841–10843.

(14) Stoeck, U.; Senkovska, I.; Bon, V.; Krause, S.; Kaskel, S. Assembly of metal-organic polyhedra into highly porous frameworks for ethene delivery. *Chem. Commun*. **2015**, 51, 1046−1049.

(15) Li, J. R.; Timmons, D. J.; Zhou, H. C. Interconversion between molecular polyhedra and metal-organic frameworks. *J. Am. Chem. Soc*. **2009**, 131, 6368−6369.

(16) Li, J. R.; Zhou, H. C. Metal-organic hendecahedra assembled from dinuclear paddlewheel nodes and mixtures of ditopic linkers with 120 and 90° bend angles. *Angew. Chem. Int. Ed.* **2009**, 121, 8617−8620.

(17) Zhao, X.; Mao, C. Y.; Bu, X. H.; Feng, P. Y. Direct observation of two types of proton conduction tunnels coexisting in a new porous indium-organic framework. *Chem. Mater*. **2014**, 26, 2492−2495.

(18) Ye, Y. X.; Guo, W. G.; Wang, L. H.; Li, Z. Y.; Song, Z. J.; Chen, J.; Zhang, Z. J.; Xiang, S. C.; Chen, B. L. Straightforward loading of imidazole molecules into metal-organic framework for high proton conduction. *J. Am. Chem. Soc.* **2017**, 139, 15604−15607.

(19) Ye, Y. X.; Zhang, L. Q.; Peng, Q. F.; Wang, G. E.; Shen, Y. C.; Li, Z. Y.; Wang, L. H.; Ma, X. L.; Chen, Q. H.; Zhang, Z. J.; Xiang, S. C. High anhydrous proton conductivity of imidazole-loaded mesoporous polyimides over a wide range from subzero to moderate temperature. *J. Am. Chem. Soc.* **2015**, 137, 913−918.

(20) Zhao, S. N.; Zhang, Y.; Song, S. Y.; Zhang, H. J. Design strategies and applications of charged metal organic frameworks. *Coord. Chem. Rev*. **2019**, 398, 113007.

(21) Nagarkar, S. S.; Unni, S. M.; Sharma, A.; Kurungot, S.; Ghosh, S. K. Two-in-one: inherent anhydrous and water-assisted high proton conduction in a 3D metal-organic framework. *Angew. Chem. Int. Ed*. **2014**, 53, 2638–2642.

(22) Su, X. L.; Yao, Z. Z.; Ye, Y. X.; Zeng, H.; Xu, G.; Wu, L.; Ma, X. L.; Chen, Q. H.; Wang, L. H.; Zhang, Z. J.; Xiang, S. C. 40-Fold enhanced

intrinsic proton conductivity in coordination polymers with the same proton-conducting pathway by tuning metal cation nodes. *Inorg. Chem.* **2016**, 55, 983−986.

(23) Dolomanov, O. V.; Bourhis, L. J.; Gildea, R. J.; Howard, J. A. K.; Puschmann, H. OLEX2: a complete structure solution, refinement and analysis program. *J. Appl. Crystallogr.* **2009**, 42, 339−341.

(24) Palatinus, L.; Chapuis, G. SUPERFLIP - a computer program for the solution of crystal structures by charge flipping in arbitrary dimensions. *J. Appl. Crystallogr.* **2007**, 40, 786−790.

(25) Sheldrick, G. A short history of SHELX. *Acta Crystallogr. Sect. A: Found. Crystallogr.* **2008**. 64, 112−122.

(26) Sarkisov, L. A. Harrison, computational structure characterisation tools in application to ordered and disordered porous materials. *Mol. Simul.* **2011**, 37, 1248−1257.

(27) Spek, A. Single-crystal structure validation with the program PLATON. *J. Appl. Crystallogr.* **2003**, 36, 7−13.